Research Article

Journal of PeptideScience

Received: 19 August 2011 Revised: 16 October 2011 Accepted: 23 October 2011 Published online in Wiley Online Library: 8 March 2012

(wileyonlinelibrary.com) DOI 10.1002/psc.1432

Sensitivity of tumor cells towards CIGB-300 anticancer peptide relies on its nucleolar localization

Yasser Perera,[a]* Heydi C. Costales,[a] Yakelin Diaz,[a] Osvaldo Reyes,[b] Hernan G. Farina,[c] Lissandra Mendez,[a] Roberto E. Gómez,[d] Boris E. Acevedo,[a] Daniel E. Gomez,[c] Daniel F. Alonso[c] and Silvio E. Perea[a]

CIGB-300 is a novel anticancer peptide that impairs the casein kinase 2-mediated phosphorylation by direct binding to the conserved phosphoacceptor site on their substrates. Previous findings indicated that CIGB-300 inhibits tumor cell proliferation *in vitro* and induces tumor growth delay *in vivo* in cancer animal models. Interestingly, we had previously demonstrated that the putative oncogene B23/nucleophosmin (NPM) is the major intracellular target for CIGB-300 in a sensitive human lung cancer cell line. However, the ability of this peptide to target B23/NPM in cancer cells with differential CIGB-300 response phenotype remained to be determined. Interestingly, in this work, we evidenced that CIGB-300's antiproliferative activity on tumor cells strongly correlates with its nucleolar localization, the main subcellular localization of the previously identified B23/NPM target. Likewise, using CIGB-300 equipotent doses (concentration that inhibits 50% of proliferation), we demonstrated that this peptide interacts and inhibits B23/NPM phosphorylation in different cancer cell lines as evidenced by *in vivo* pull-down and metabolic labeling experiments. Moreover, such inhibition was followed by a fast apoptosis on CIGB-300-treated cells and also an impairment of cell cycle progression mainly after 5 h of treatment. Altogether, our data not only validates B23/NPM as a main target for CIGB-300 in cancer cells but also provides the first experimental clues to explain their differential antiproliferative response. Importantly, our findings suggest that further improvements to this cell penetrating peptide-based drug should entail its more efficient intracellular delivery at such subcellular localization. Copyright © 2012 European Peptide Society and John Wiley & Sons, Ltd.

Supporting information can be found in online version of this article

Keywords: CIGB-300; CK2; B23/nucleophosmin; P15-Tat; cell penetrating peptide

Introduction

CIGB-300 is a novel anticancer peptide selected to impair the casein kinase 2 (CK2)-mediated phosphorylation by direct binding to the conserved phosphoacceptor site on their substrates [1], hence differing from more conventional ATP-competitive or non-competitive small molecule inhibitors that target the enzyme *per se* [2]. The enzyme CK2 is a highly conserved ser/threo protein kinase, which is constitutively active and usually overexpressed in tumor cells sustaining the neoplastic transformation through the regulation of proliferative, survival, and stress pathways [3,4]. Based on such epidemiological findings and a huge body of pre-clinical experimentation, CK2 has been recently coined as an example of a non-oncogene addiction in cancer cells [5].

CIGB-300, formerly known as P15-Tat, is composed of a phosphorylation inhibitor domain (P15) fused to the widely used cell penetrating peptide (CPP) Tat [6] through a βAla spacer, which provides to the peptide chimera the required conformational flexibility to interact with its target (Figure 1). P15 inhibitor peptide was initially isolated by screening a random cyclic peptide phage display library using the conserved acidic fosfoaceptor domain for CK2 on the HPV-16 E7 oncogenic protein as a model substrate [1]. In consideration with the high degree of conservation for the CK2-phosphoaceptor domain among more than 300 validated substrates [7] in principle, CIGB-300 may target several CK2 substrates by direct binding to such domain, thus impairing its phosphorylation by the kinase.

Interestingly, our previous findings suggested that the multifunctional nucleolar protein B23/nucleophosmin (NPM), which is frequently overexpressed, mutated, or rearranged in neoplastic tissues [8], might be the major intracellular target for CIGB-300 [9]. In a model cancer cell line, CIGB-300 interacted with B23/NPM at the cell nucleolus, impairing its CK2-mediated phosphorylation and inducing a fast apoptotic cell death, a cellular outcome that

* *Correspondence to: Yasser Perera Negrin, Laboratory of Molecular Oncology, Division of Pharmaceuticals, Center for Genetic Engineering and Biotechnology (CIGB), Ave 31 e/ 158 and 190, Havana, CP10600, Cuba. E-mail: yasser.perera@cigb.edu.cu*

a *Laboratory of Molecular Oncology, Division of Pharmaceuticals, Center for Genetic Engineering and Biotechnology (CIGB), Havana, CP10600, Cuba*

b *Peptide Synthesis Group, Chemical-Physical Division, Center for Genetic Engineering and Biotechnology (CIGB), Havana, CP10600, Cuba*

c *Laboratory of Molecular Oncology, Quilmes National University, R. Sáenz Peña 352, Buenos Aires, Bernal, B1876BXD, Argentina*

d *ELEA Laboratories, Sanabria 2353, Buenos Aires, C1417 AZE, Argentina*

Abbreviations used: *B23/NPM, nucleophosmin; CK2, casein kinase 2; IC_{50}, concentration that inhibits 50% of proliferation; CPP, cell penetrating peptide*

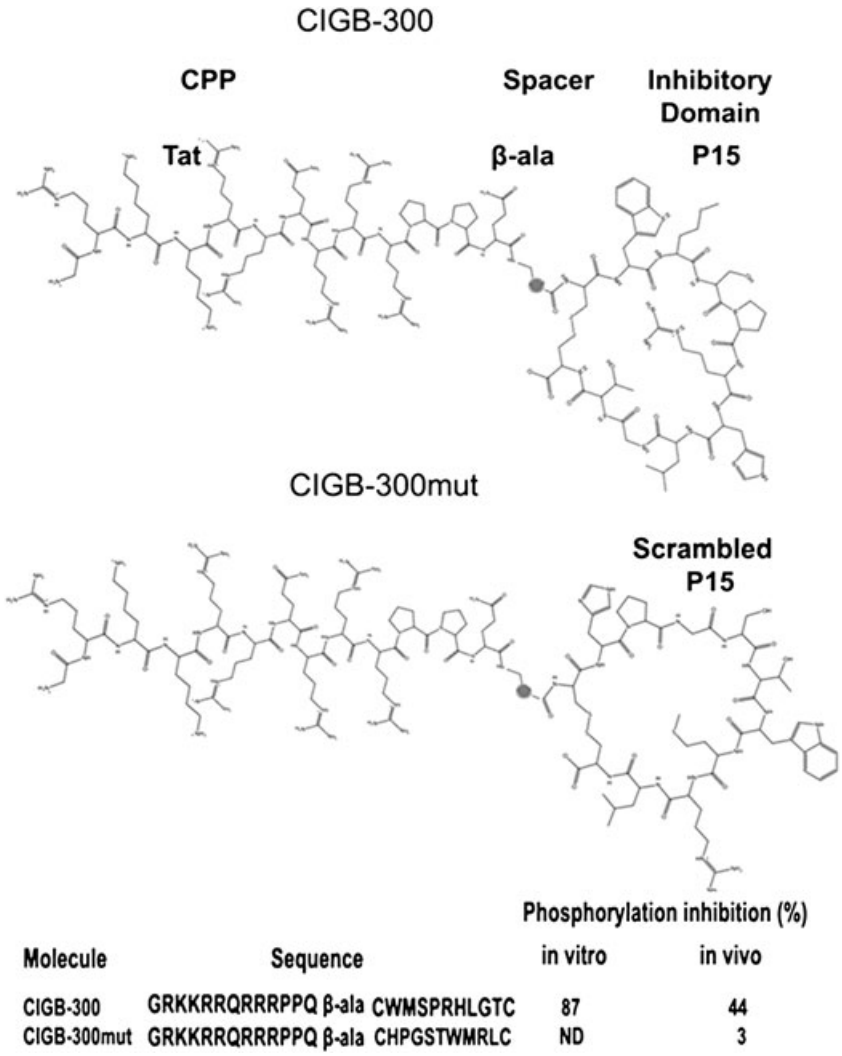

Molecule	Sequence	Phosphorylation inhibition (%) in vitro	in vivo
CIGB-300	GRKKRRQRRRPPQ β-ala CWMSPRHLGTC	87	44
CIGB-300mut	GRKKRRQRRRPPQ β-ala CHPGSTWMRLC	ND	3

Figure 1. Chemical structure of CIGB-300 and its scrambled version CIGB-300mut. The peptide CIGB-300 is composed of the polycationic cell penetrating peptide Tat fused to the phosphorylation inhibitor domain P15 through a βAla spacer. P15 domain, which is constrained by a disulfide bridge, includes hydrophobic amino acid residues (i.e. W, M, L) and positively charged amino acid residues (i.e. R, H), which confers at physiological pH a net charge of +2. The figure also shows the inhibitory effect of CIGB-300 (100 μM) over the casein kinase 2-mediated phosphorylation on B23/NPM both *in vitro* and *in vivo* in a model cancer cell line (data from reference [9]) as well as the effect of the equivalent concentration of the scrambled peptide CIGB-300mut.

seems to be preceded by the nucleolar disassembly. However, if such impairment on B23/NPM phosphorylation could also explain the differential antiproliferative activity observed for CIGB-300 in diverse tumor types [1,10], remains to be determined. Moreover, considering that CIGB-300 relies on a CPP for its internalization in tumor cells, the successful interaction of the peptide with B23/NPM or any other potential CK2 substrate implies that it should reach efficiently the target in a particular cellular compartment [11]. Particularities of such internalization processes on each cell line may also account for the observed differences in the antiproliferative response towards CIGB-300 in cancer cell lines [1,10].

Here, we evidenced that CIGB-300 antiproliferative activity correlates with its nucleolar localization, the main subcellular localization for the previously identified B23/NPM target. CIGB-300 interacted with and disturbed the CK2-mediated phosphorylation of B23/NPM with the subsequent induction of apoptosis and cell cycle arrest on treated cells, both cellular outcomes contributing to the observed antiproliferative effect. The findings outlined in this work validate B23/NPM as a major target for CIGB-300 and also indicate that subcellular localization of CIGB-300 at the cell nucleolus of tumor cells is a crucial event that dictates its antiproliferative effect.

Materials and Methods

Cell Lines and Cultures

The mycoplasm-free human cell lines derived from lung (NCI-H460, NCI-H125, NCI-H82, A549), cervix (SiHa, HeLa, HEp-2C, CaSki), prostate (PC-3, DU 145, LNCaP), and colon cancer (SW948, HT-29, LS 174T) were originally acquired from American Type Culture Collection (Rockville, MD, USA). Non-tumorogenic human lung fibroblast (MRC-5) and monkey kidney (Vero) cell lines were also acquired from American Type Culture Collection, whereas the spontaneously transformed keratinocyte cell line (HaCaT) was obtained from Cell Lines Service (CLS, Eppelheim, Germany). All cell lines were routinely cultured in Roswell Park Memorial Institute medium 1640 or Dulbecco's Modified Eagle's medium (Invitrogen, Carlsbad, CA, USA), supplemented with 10% fetal bovine serum (FBS; PAA, Ontario, Canada) and gentamicin (Sigma, St. Louis, USA). Metabolic

Journal of PeptideScience

labeling experiments were carried out in phosphate-free Dulbeccoís Modified Eagleís medium, supplemented with the indicated percentage of FBS. Cell lines were routinely tested according to Cell Line Verification Test Recommendations [12] to verify at least three of the proposed parameters.

Peptide Synthesis

All peptides used in this work were synthesized as previously described [1]. The CIGB-300-F and CIGB-300-B conjugates were obtained through amide linkage between the N-terminal Gly amino acid residue from CIGB-300 and the reagents carboxyfluoresceine (Sigma, USA) or 7-NHS-biotin (Merck, Darmstadt, Germany), respectively. The identity of all peptides was confirmed by ion-spray mass spectrometry (Micromass, Manchester, United Kingdom).

Sulforhodamine B Assay and Data Analysis

Antiproliferative assays were essentially performed as described previously [13]. Relative log IC_{50} was estimated using the following formula: relative log IC_{50} = mean log IC_{50} (panel) – log IC_{50} (cell line). Dose–response curves were fitted using the software Calcusyn (Biosoft, Cambridge, UK), and simulated curves were visualized using the software GraphPad Prims v4 (GraphPad Software, San Diego California, USA).

Pull-down, Western Blot and Metabolic Labeling

Cells were seeded at 3×10^5 cells/ml and cultured for 20 h. Next day, the CIGB-300-B was added and incubated for 10 min. Subsequently, cells were collected by centrifugation, washed twice with cold phosphate-buffered saline (PBS), and lysed in hypotonic PBS solution containing 1 mM of dithiothreitol (Sigma, USA) and Complete inhibitor (Roche, Indianapolis, IN, USA) by five freeze–thaw cycles. Then, cellular lysates were cleared by centrifugation at 12 000 r.p.m. 4 °C for 15 min and 300 μg of total proteins added to 50 μl of pre-equilibrated Streptavidin Sepharose matrix (Amersham, Uppsala, Sweden). After 1 h of incubation at 4 °C, the matrix was collected by short spin, extensively washed with PBS 1 mM dithiothreitol, and bound proteins eluted by boiling in Laemmli Buffer.

Protein samples from pull-down experiments or from total cell lysates were resolved in conventional SDS-PAGE gels [14], transferred to nitrocellulose membranes (Hybond-C extra, Amershan, Little Chalfont, UK), and submitted to western blot experiments using 1 μg/ml Mab anti-B23 clone FC-61991 (Invitrogen, USA) or Mab anti-β-actin clone AC-15 (1 : 1000) (Sigma, USA). Fluorescent signal was developed using luminol (Sigma, USA) and registered on X-ray films (Ortho CP-G plus, Belgium).

For *in vivo* [^{32}P] *ortho*-phosphate labeling, cell cultures were grown in Roswell Park Memorial Institute medium at 10% FBS for 20 h. In the next day, cells were incubated in phosphate-free medium supplemented with 10% FBS for 1 h. The medium was replaced by fresh one containing 1 mCi/ml of [^{32}P] *ortho*-phosphate (Amersham, UK) and 5% FBS, and cells were maintained under such conditions for 30 (NCI-H125, HEp-2C, SiHa and PC-3) or 120 min (SW948) to achieve labeling of proteins. Subsequently, selected peptides or the CK2 inhibitor 4, 5, 6, 7-tetrabromobenzotriazole were added and incubated for 30 min or 2 h. Then, cells were washed and lysed with RIPA buffer containing 2 mmol/L of phosphatase inhibitors NaF, Na_3VO_4, and β-glycerophosphate (Sigma, USA). Lysates were clarified and supernatants collected for immunoprecipitation. For each reaction, 200 μg of total proteins were mixed with 3 μg of the anti-B23 antibody. Subsequent steps were performed as recommended in the protein G immunoprecipitation kit (Sigma, USA). Finally, immunoprecipitates were analyzed by SDS-PAGE and gels were blue-stained, dried, and further exposed. Image analysis from the X-ray films and gels was performed with ImageJ 1.37v (NIH, Bethesda, Maryland, USA). Immunoprecipitation efficiency and gel loading were normalized by dividing the [^{32}P] signal by their corresponding blue-stained protein signal for each lane.

Apoptosis Assays

Radioactive DNA-laddering assays were performed essentially as described in the website (http://www.celldeath.de/apometh/dnafragm.html). Fragmentation percentage was estimated according to the following formula: (%) = [cpm (untreated) − cpm (treated)] / cpm (untreated) × 100. Annexin V staining was performed using Annexin V-FITC apoptosis detection kit according to instructions from manufacturer (BD PharMingen, San Diego, CA, USA). Subsequently, flow cytometry analysis was carried out on Particle Analysing System-III flow cytometer using their proprietary software FloMax v2.4f (PARTEC, Münster, Germany). For representation purposes, the software WinMDI v. 2.8 (http://facs.scripps.edu/software.html) was also used.

Cell Cycle Analysis

Cell cultures were incubated with equipotent doses of CIGB-300 or PBS for 0.5, 1, 3, 5, 8 and 24 h at 37 °C and 5% CO_2. Subsequently, cells were collected by trypsinization, washed, and fixed with ice-cold methanol/acetone (4 : 1) at 4 °C for 1 h. The cells were stained for 20 min at 37 °C in the dark by incubation with propidium iodide solution (100 μg/ml) and 10 μg/ml of DNase-free RNase and subsequently analyzed by flow cytometry.

Flow Cytometry and Fluorescence Microscopy

Peptide internalization was studied at 3, 10, 30, and 60 min after addition of 100 μM of CIGB-300-F conjugate. Briefly, 350 000 cells were seeded in six well plates and incubated for 18–20 h. Subsequently, the culture medium was replaced, CIGB-300-F added, and plates incubated during selected times. Following PBS washes, the cells were extensively trypsinized and resuspended in PBS solution containing 5 μg/ml propidium iodine (Sigma, USA). Flow cytometry analysis was performed on the earlier mentioned instrument. Fluorescent emission was registered by FL1 channel (520 nm, fluorescein) and FL3 channel (630 nm, propidium iodine). Cross-talk compensation between was carried out post-acquisition and individually for each sample.

Fluorescence microscopy experiments were performed on an Axioskop 40 instrument (Carl Zeiss, MN, USA) equipped with a UV lamp (HBO 50/AC) and a digital camera (PowerShot G6, Canon, Japan). Briefly, cell suspensions of 3×10^5 cells/ml were cultivated for 16–20 h in suitable cell culture chambers at 37 °C and 5% CO_2. In the next day, the CIGB-300-F or CPP-F conjugates were added to the cell cultures at final concentrations of 50, 100, or 200 μM and incubated for 3, 10, 30, and 60 min. Afterwards, the cells were fixed for 15 min with paraformaldehyde 4% (Sigma, USA), washed with PBS, and mounted in 40% glycerol (Plusone, Uppsala, Sweden). Finally, fixed cells were immediately analyzed by fluorescence microscopy.

Statistical Analysis

To analyze the differences in nucleolar counts (% nucleoli+) among the cell lines, one-way analysis of variance and Tukey's multiple comparison post-test were performed. Moreover, a Pearson correlation calculation was carried out to correlate antiproliferative effect to % nucleoli+ using the GraphPad Software.

Results

Antiproliferative Effect of CIGB-300 on Cancer Cells

The antiproliferative effect of CIGB-300 in a panel of human cancer cell lines derived from four tumor types was evaluated using the Sulforhodamine B-based assay (Figure 2a, b and c). In parallel, to assess the selectivity of CIGB-300 against cancer cells, the peptide was also tested in four non-tumorogenic cell lines (Figure 2a and d).

CIGB-300 exerted a broad antiproliferative effect in the micromolar range (20–300 μM) in cells derived from lung, cervix, prostate, and human colon cancers, although lung cancer cells seemed to be particularly sensitive (mean $IC_{50} = 60$ μM, range: 20–120 μM) (Figure 2a and b; Table 1). Otherwise, CIGB-300 showed nearly two-fold lower potency in non-tumorogenic cell lines (mean $IC_{50} = 190$ μM) than in tumor cells (mean $IC_{50} = 100$ μM).

To assess the potential unspecific contribution of the Tat CPP moiety to the antiproliferative effect seen on each cell line, we evaluated its cytotoxicity in the same experimental setting. Tat peptide exerted a significant effect only at doses above 200 μM in most of the cell lines tested, although nearly 15% of cytotoxic effect was observed at 100 μM in cell lines HEp-2 and SW948 (Table 1; Figure S1, see Supporting Information). Interestingly, the cytotoxic effect estimated for a CIGB-300 mutant peptide (CIGB-300mut), which previously failed to inhibit the *in vivo* CK2-mediated phosphorylation on B23/NPM, was even milder than the CPP alone in three of the five cell lines tested (Table 1).

CIGB-300 Interacts with B23/NPM and Inhibits its CK2-mediated Phosphorylation

To verify if CIGB-300 interacts with B23/NPM in five cancer cell lines representing four different tumor types and response phenotypes, we conducted *in vivo* pull-down and metabolic labeling experiments using equipotent doses of CIGB-300 (IC_{50}, Table 1) (Figure 3a, b and d). Immunobloting data indicated that initial B23/NPM protein levels in cell extracts submitted to pull-down experiments were quite similar in the cell lines tested and that such protein was efficiently pulled down by biotinylated CIGB-300 (CIGB-300-B) after 10 min of incubation (Figure 3a). Moreover, after 30 min, equipotent CIGB-300's doses inhibited B23/NPM phosphorylation nearly to 50% in NCI-H125, SiHa, and PC-3 cell lines (Figure 3b), whereas less inhibition was achieved in HEp-2C (33%) and SW948 (16%) cell lines only after 2 h of treatment (Figure 3d).

In the same experimental setting, we also tested the effect of 100 μM of CIGB-300 on B23/NPM phosphorylation in NCI-H125 and SiHa cells. Such a dose can be considered more potent for NCI-H125 cell line but suboptimal for SiHa cells according to its antiproliferative effect (Table 1). Interestingly, a similar inhibitory effect over the CK2-mediated phosphorylation was obtained for NCI-H125 but not in SiHa cells, whereas identical doses of the CIGB-300mut peptide, which lacks significant antiproliferative activity, did not show any inhibition (Figure 3c).

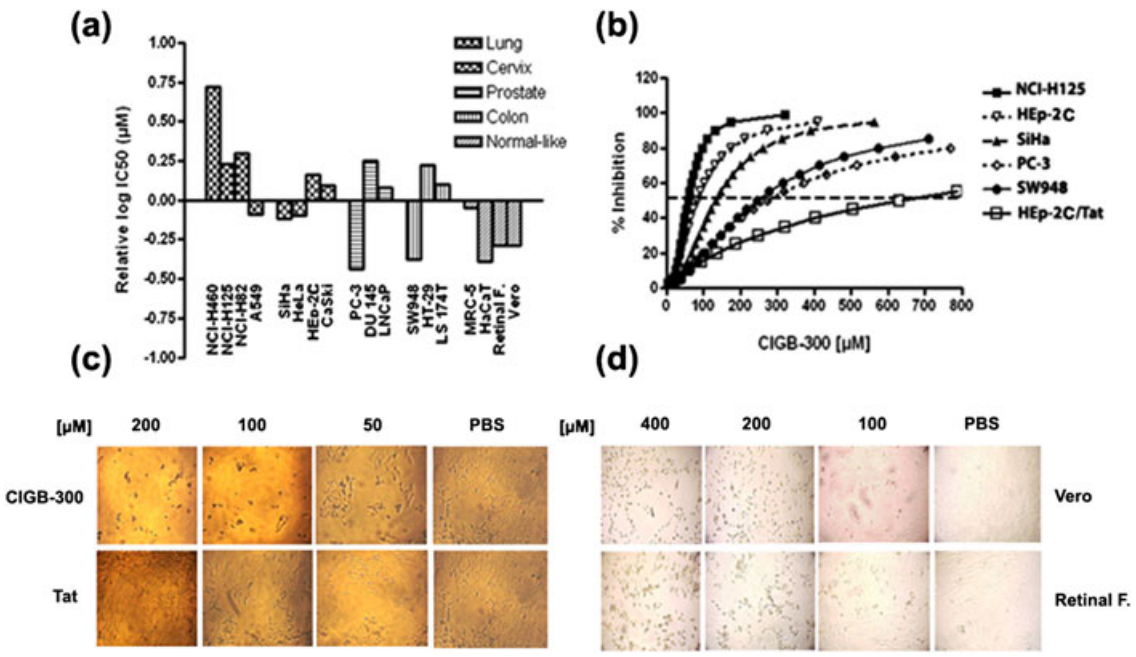

Figure 2. CIGB-300's antiproliferative effect in human cell lines derived from four different tumor localizations or from non-tumorogenic tissues. (a) CIGB-300 response profile generated using mean IC_{50} across all cell lines as baseline (123 μM); negative log IC_{50} values correspond to cell lines with lower sensitivity than average, and positive log IC_{50} values represent cell lines that are more sensitive than average. (b) Antiproliferative dose–response curves for CIGB-300 in five selected cancer cell lines. CIGB-300 peptide at concentrations ranging from 400 to 10 μM was incubated for 48 h, and their effect in tumor cells estimated by the sulforhodamine method. (c and d) Effect of CIGB-300 in the lung cancer cell line NCI-H125 (c) or two non-tumorogenic cells lines (d) using light microscopy (magnification 10×). The antiproliferative effect of the Tat CPP alone in HEp-2C (b) and NCI-H125 (c) is also shown.

Journal of PeptideScience

Table 1. Parameters estimated from the fitted dose–response antiproliferative curves for CIGB-300 and control peptides (Tat and CIGB-300mut) in five selected cancer cell lines. The curves were fitted to the median-effect equation using the software Calcusyn.

		CIGB-300				Tat	CIGB-300mut*
Cell line	Origin	IC_{50}	*m*	*r*	IC_X	IC_{50}	IC_{50}
NCI-H125	Lung	59 ± 4	2.70	0.99	79 ± 3	2124	581
HEp-2	Cervical	70 ± 13	1.82	0.96	64 ± 2	630	292
SiHa	Cervical	134 ± 3	2.00	0.95	37 ± 4	1876	<<400
PC-3	Prostate	280 ± 8	1.34	0.95	21 ± 7	1120	<<400
SW948	Colon	239 ± 42	1.63	0.97	21 ± 9	4302	<<400

IC_{50}, CIGB-300's concentration that inhibits 50% the cellular proliferation (μM); *m*, steepness of the dose–response curve; *r*, quality of the fitness to the median-effect equation; IC_X, antiproliferative effect level corresponding to 100 μM of CIGB-300.

* For CIGB-300mut, no inhibition was observed at concentrations below 400 μM in three of the five cell lines; therefore, the corresponding IC_{50} could not be estimated.

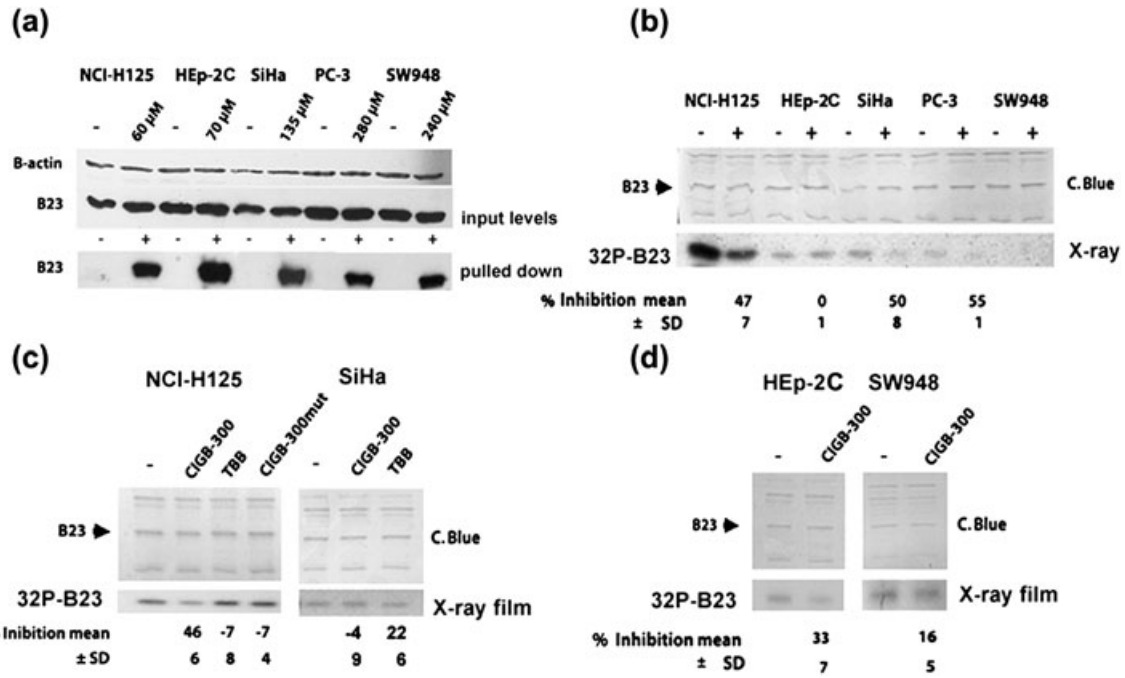

Figure 3. CIGB-300 at equipotent doses binds to B23/NPM *in vivo* and impairs its phosphorylation in five cancer cell lines from different origins. (a) Western blot analysis of B23/NPM protein levels (~34 kDa) in total cell extracts derived from CIGB-300-treated or untreated cells (−) for 30 min with peptide concentrations corresponding to the IC_{50} for each cell line (upper panel). β-actin protein levels were used to normalize cell extract load/lane. Cell cultures were incubated with the same concentrations of CIGB-300-biotin conjugate (+) or left untreated (−) for 10 min, submitted to pull-down experiments, and B23/NPM identified in the precipitated fraction through immunobloting (lower panel). (b) [^{32}P] metabolic labeling performed in the five cell lines to estimate the B23/NPM phosphorylation inhibition exerted by the CIGB-300 at the IC_{50} dose after 30 min of incubation. Upper panel shows the coomassie blue-stained SDS-PAGE gel from the B23/NPM immunoprecipitation reaction where also two bands corresponding to the light (25 kDa) and heavy (55 kDa) chains from the anti-B23/NPM Mab are noted. Lower panel shows the [^{32}P] exposed X-ray films from the dried SDS-PAGE. The amount of B23/NPM phosphorylation inhibition (%) was estimated using untreated cells as reference (100% phosphorylation) and the B23/NPM protein load/lane for normalization as described in Materials and Methods. (c) [^{32}P] metabolic labeling experiments performed in the cell lines NCI-H125 and SiHa with 100 μM of CIGB-300, tetrabromobenzotriazole, or a CIGB-300 derivative that lacks antiproliferative activity (CIGB-300mut), all incubated for 30 min. (d) Similar experiments to (b) were conducted in HEp-2C and SW948 cell lines but using longer incubation with CIGB-300 (2 h) or [^{32}P] labeling time for SW948 (2.30 h).

B23/NPM Phosphorylation Impairment Leads to Apoptosis but also Impacts on Cell Cycle

Previously, we demonstrated that the impairment of the CK2-mediated phosphorylation on B23/NPM precedes the onset of a fast apoptotic cell death [9]. Therefore, we analyzed the putative apoptosis induction by CIGB-300 in the five cancer cell lines after 30 and 120 min of treatment using Annexin V and genomic DNA fragmentation assay, respectively (Figure 4a and b).

Equipotent doses of CIGB-300 induced an early apoptosis in 10% to 35% of cell populations from all the cell lines (normalized to untreated cells) as determined with the Annexin V assay. Further incubation for 6 hrs increases the apoptotic cell populations to 26% and 47% in PC-3 and SW948, respectively (data not shown). Moreover, a clear dose-related apoptosis induction was evidenced in NCI-H125 and SiHa cells after 2 h of incubation with CIGB-300 using DNA-laddering assay (Figure 4b).

On the other hand, we also evaluated the impact of B23/NPM phosphorylation inhibition on cell cycle distribution. Equipotent CIGB-300's doses were added to cell cultures in time-course experiments, and the cells were subsequently analyzed for DNA content by flow cytometry. Interestingly, data from NCI-H125, SiHa, Hep-2C,

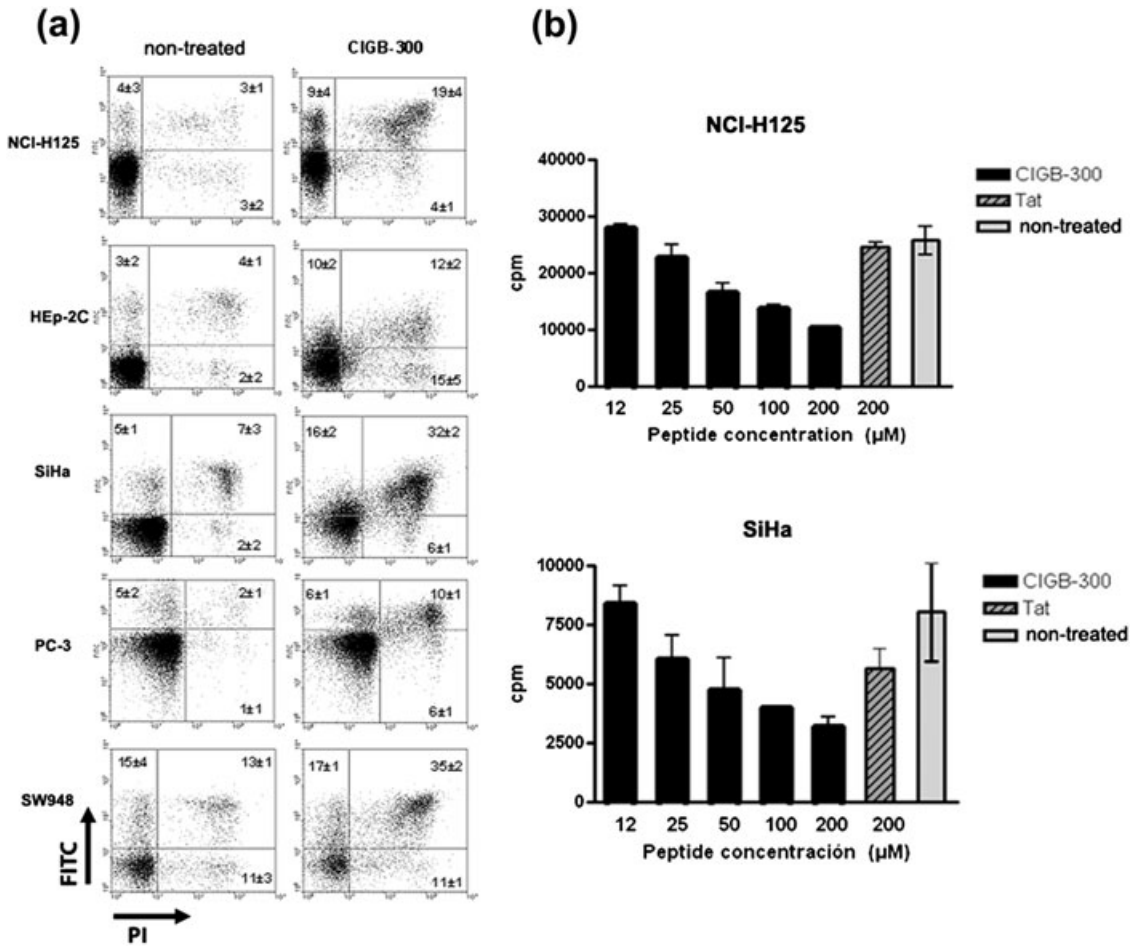

Figure 4. CIGB-300 induces a fast and dose-dependent apoptosis in cancer cells. (a) Annexin V staining (FITC) revealed by flow cytometry analysis in cancer cells treated for 30 min with CIGB-300 doses corresponding to the IC_{50} for each cell line. Propidium iodine (PI) was used as a non-vital fluorescent dye to exclude necrotic cells (FITC- / PI+), apoptotic or late apoptotic cells were scored as FITC+ or FITC+/PI+ cells, respectively. Numbers refer to percent of each population for marked cells (mean ± SD). (b) NCI-H125 or SiHa cells were incubated with peptide concentrations ranging from 12 to 200 μM for 2 h, and the DNA fragmentation was estimated by the radioactive method. DNase I digestion was used as a positive control, and PBS to assess spontaneous apoptosis (non-treated cells). Columns, means from three replicates; bars, SD. Radioactivity counts per min (cpm) were performed using a beta counter.

and PC-3 cell lines indicated that cell populations accumulate at different phases mainly after 5 h of treatment, whereas no significant changes in cell cycle distribution were detected in SW948 (Figure 5a and b).

Subcellular Localization but Not Internalization Levels of CIGB-300 Correlates with its Antiproliferative Activity

To evaluate how CIGB-300's internalization levels could be associated with its antiproliferative effect, we performed flow cytometry analysis using a CIGB-300-fluorescein conjugate (CIGB-300-F). The peptide was rapidly internalized in 70% to 98% of the cells with higher transduction levels reached after 10 min of incubation for all cell lines (Figures 6a and S2, see Supporting Information). Correspondingly, CIGB-300-F accumulation also increased up to 10 min of incubation although maximum peptide levels clearly differed among cell lines (Figure 6b). Interestingly, higher and faster peptide accumulation was registered in less sensitive PC-3 cell line, whereas an inverse picture was observed for the most sensitive NCI-H125 cell line (Figure 6b; Table S3, see Supporting Information). Of note, peptide internalization was similar for HEp-2C, SiHa, and SW948 cell lines despite their quite different response phenotype.

On the other hand, the subcelullar distribution of CIGB-300-F was analyzed by fluorescence microscopy. A diffuse fluorescent pattern was observed throughout the cell at all the incubation times (cytoplasmic and nuclear region) but mainly localized to nucleoli (Figure 7, lower panel). Such pattern was more evident in NCI-H125, HEp-2C, and SiHa cells, whereas incubation with a conjugated peptide that lacks the CPP moiety (CPP-) at the same concentration only results in a weak extracellular fluorescence (Figure 7, middle panel).

To quantitatively document the observed differences among cell lines, the number of cells displaying nucleolar fluorescence (nucleoli+ cells) was counted. Interestingly, cell lines NCI-H125 and HEp-2C showed the highest values with 80% and 70% of nucleoli+ at 10 min of incubation, respectively (Figure 8a), whereas SW948 displayed less than 20%. Furthermore, at least for NCI-H125 and SiHa cells, the rate of nucleoli+ cells was dose-related, whereas the fluorescent peptide CPP- used as negative control did not internalize at all (Figure 8b).

Taking into account that the most sensitive tumor cell lines displayed higher nucleolar deposit of CIGB-300, we attempted to correlate the estimated antiproliferative effect with such subcellular distribution. A significant correlation between these two variables were obtained for all cell lines using one peptide

Journal of PeptideScience

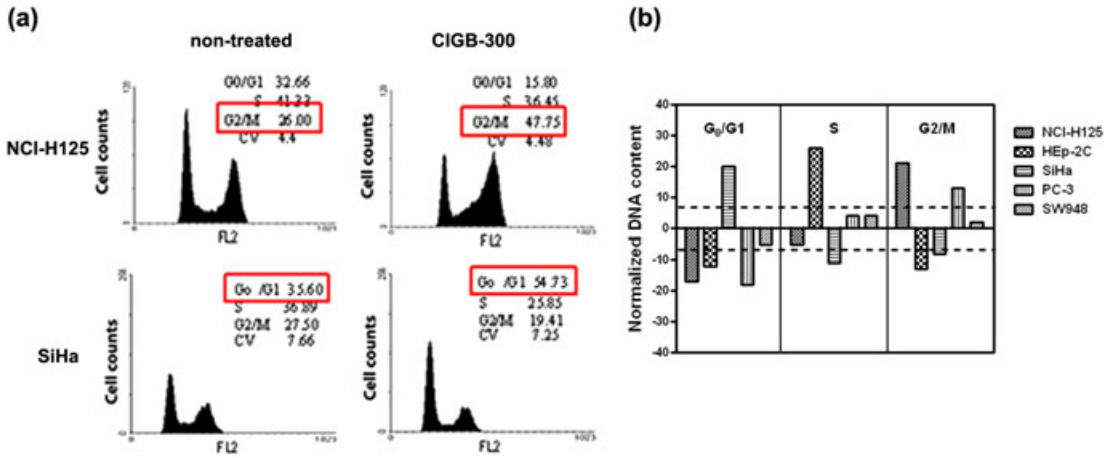

Figure 5. Cell cycle distribution of exponentially growing cell cultures treated with equipotent doses (IC_{50}) of CIGB-300. (a) Flow cytometry histograms of DNA content form NCI-H125 or SiHa cells treated for 5 h with CIGB-300 using propidium iodine as a fluorescent mark. Non-treated cells were used as a reference for unperturbed progression through the cell cycle. Percentage of cells at different phases of the cell cycle was estimated using the FloMax software. (b) Graph summarizing the cell cycle distribution of the five cell lines according to the normalized DNA content = % population phase × [CIGB-300-treated cells] − % population phase × [non-treated cells] where a positive value represent the arrest of population at a particular cell cycle phase with respect to the time-matched untreated culture (5 h). Dashed line represents a cut-off of significance. All the experiments were performed at least in triplicate.

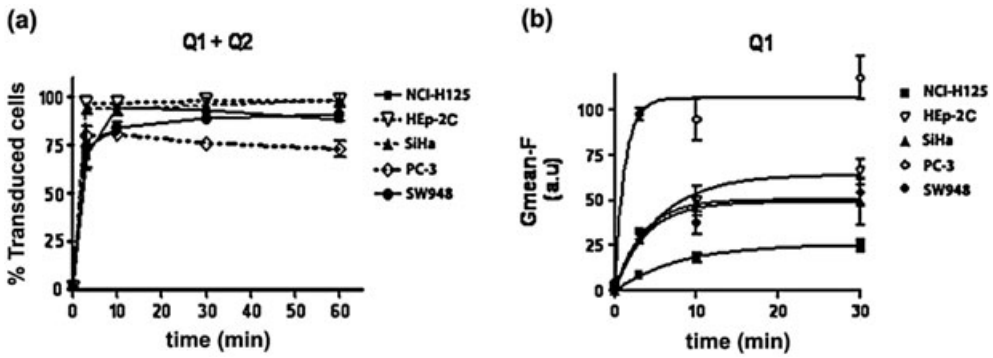

Figure 6. Internalization kinetics of CIGB-300 in five tumor cell lines measured by flow cytometry. CIGB-300 conjugated to fluorescein was added at 100 μM and incubated for 3, 10, 30 and 60 min. Subsequently, the cells were trypsinized, washed, and analyzed using propidium iodine as a second stain to exclude damaged/dead cells. (a) Percent of CIGB-300's transduced cells registered in Q1 and Q2 quadrants. (b) Intracellular accumulation of CIGB-300 measured as the geometric mean of the fluorescein emission in Q1 quadrant. Q1 quadrant: cells positive to CIGB-300 (transduced) and Q2: double positive cells (transduced and membrane-damaged cells). The detailed analysis of one representative sample is provided in Figure S2. a.u, arbitrary units.

concentration ($r = 0.83$; $p < 0.0001$) (Figure 8c) but also when different CIGB-300-F's concentrations were tested in NCI-H125 and SiHa cells ($r = 0.79$; $p < 0.0001$) (Figure 8d).

Discussion

Preliminary findings and those provided here evidenced that CIGB-300 peptide exerts a broad antiproliferative effect on cancer cells derived from four different solid tumor localizations. However, the inhibitory effects on cell proliferation clearly differ among the cell lines tested with IC_{50}'s ranging from 20–300 μM of peptide concentration. To identify the molecular and/or cellular basis that could explain such differences, we first aimed to corroborate if B23/NPM was similarly targeted by CIGB-300 in such diverse tumor cell lines. Moreover, considering that CIGB-300 is a chimeric peptide that uses the CPP Tat to achieve intracellular milieu, we also examined how internalization and subcellular distribution could determine on the observed antiproliferative effect in cancer cells.

Our results corroborated that B23/NPM is a major target for CIGB-300 in the five selected cancer cells. Pull-down experiments demonstrated that CIGB-300 at equipotent doses interacts with B23/NPM in all cell lines tested, although such interaction impinges B23/NPM phosphorylation at different levels. Of note, intrinsic B23/NPM phosphorylation levels, but not B23/NPM protein levels, seem to decrease from the most sensitive (NCI-H125) to less responder's cell lines (PC-3 and SW948). Moreover, even at CIGB-300's equipotent doses, some kinetic constraints on B23/NPM phosphorylation inhibition may also occur, considering that for HEp-2C and SW948 cell lines only after 2 h of treatment that some inhibition was seen. The impairment of the CK2-mediated phosphorylation on B23/NPM was not only accompanied by apoptosis induction on treated cells but also disturbed differentially cell cycle progression probably reflecting cell-line specific genetic traits such as the status of p53 or Rb tumor suppressors. Interestingly, for HEp-2C and SW948 cells, roughly 20% of cell population displayed early apoptosis signals despite no B23/NPM phosphorylation inhibition was registered at that time, a finding attributable to the higher cytotoxicity observed for the CPP moiety *per se* in both cell lines (Figure S1). Altogether, both cellular outcomes, apoptosis and cell cycle arrest, may contribute to the observed CIGB-300's *in vitro* antiproliferative effect.

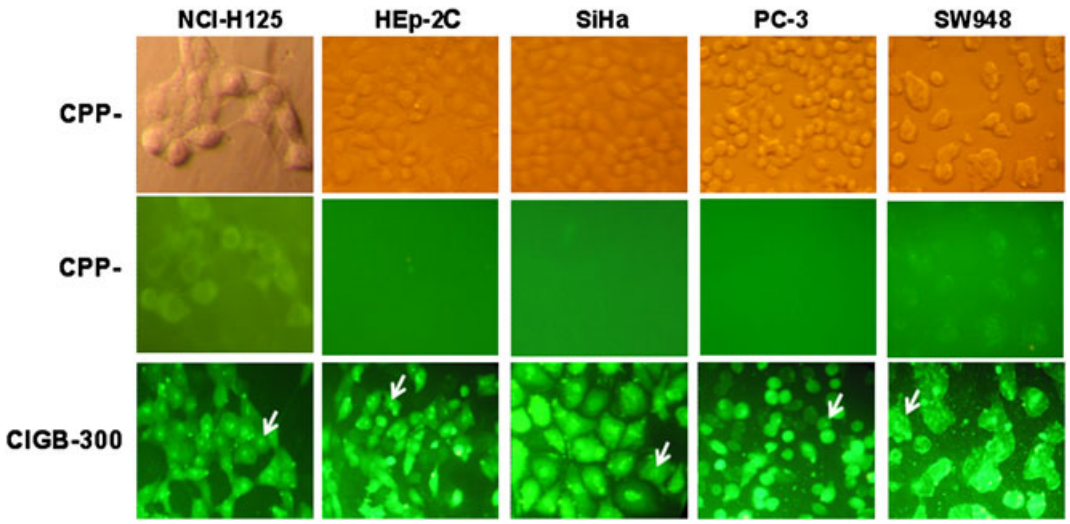

Figure 7. Subcellular localization of fluorescein-conjugated peptides revealed by fluorescence microscopy after 10 min of incubation with 100 μM of CIGB-300-F (lower panel) or a peptide conjugate that lacks the cell penetrating peptide moiety (CPP-, middle panel). Microscopy images were obtained with 20× magnification. White arrows: cell nucleoli.

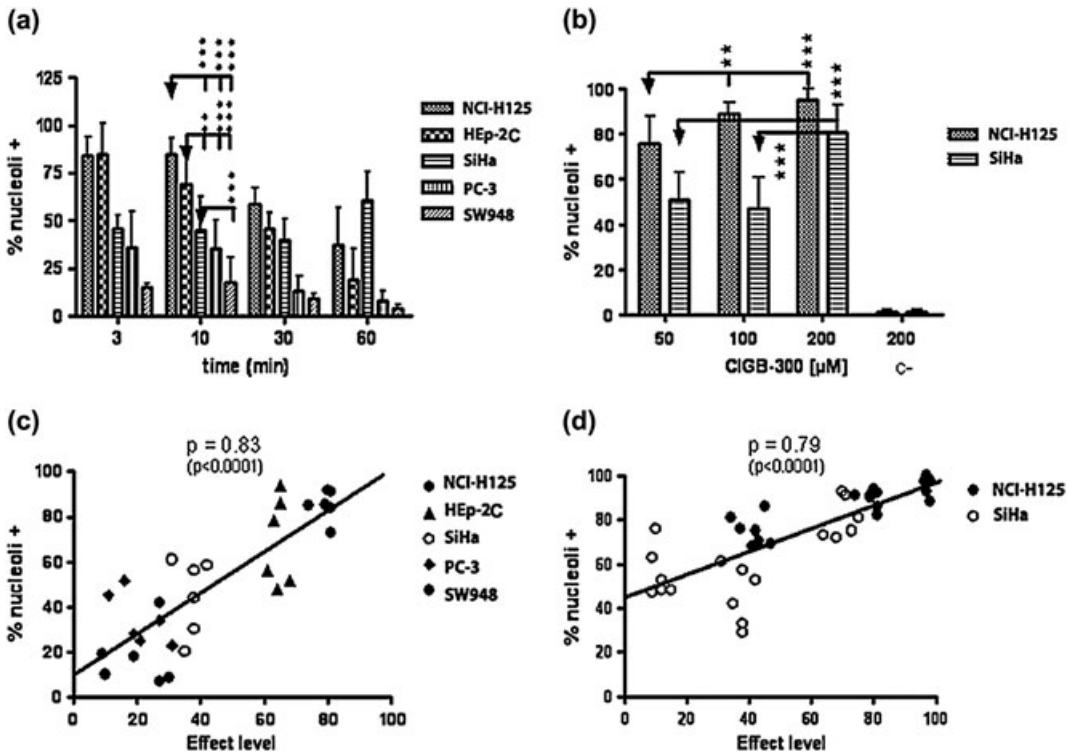

Figure 8. Correlation between nucleolar deposition and the antiproliferative effect of CIGB-300 in cancer cell lines. (a) The number of cells displaying nucleolar fluorescence in the five cell lines after incubation with 100 μM of CIGB-300-F for 3, 10, 30 and 60 min was counted and related to the total number of transduced cells (% of nucleoli+). (b) The percentage of nucleoli+ was estimated in NCI-H125 and SiHa cells after 10 min of incubation with different concentrations of CIGB-300-F. Asterisks denote the degree of significance in the statistical comparisons connected by lines (one-way analysis of variance). (c and d) The percentage of nucleoli+ for each cell line was correlated with the antiproliferative effect exerted by an identical dose of CIGB-300. The effect level was estimated interpolating the concentrations of CIGB-300 used for each assay on the simulated dose–response curves. *p*, Pearson coefficient of correlation; $p<0.0001$, statistical significance of the correlation.

Having demonstrated that CIGB-300 also target B23/NPM phosphorylation in the five selected cancer cell lines, we focused on the characterization of peptide internalization to explain the observed differential response profile. The data from flow cytometry analysis revealed that internalization of CIGB-300 in tumor cells is quite similar to those described for Tat and other CPP in terms of kinetics and efficiency of transduction [15,16]. Although the five cell lines could be classified in three distinguishable groups according to the rate and amount of peptide internalization, we did not find any obvious association between such parameters and the response phenotype. However, a clear picture emerges when the subcellular localization of the peptide was analyzed. The significant correlation

Journal of PeptideScience

found between nucleolar localization and the antiproliferative effect for CIGB-300 indicates that reaching the nucleolar compartment is crucial for the biological activity of the cargo, further suggesting that intrinsic differences among cancer cell lines can be minimized by increasing peptide dose. In line with this, when the CIGB-300-F conjugate was used at the IC_{50}'s concentrations, the number of cell displaying nucleolar fluorescence increased above 50% in four of the five cell lines (data not shown). However, at high doses (>200 μM), the peptide may also affect non-tumorogenic cells, or even the CPP *per se* could be cytotoxic. Our internalization experiments were mainly performed at 100 μM of CIGB-300, a peptide concentration where Tat only causes a minimal interference with the cellular readouts.

The advantages and limitations of the CPP as delivery vehicles have been widely discussed [17]. The CPP can efficiently deliver a wide range of biological cargos to the intracellular milieu by mechanisms that include different types of endocytosis or even a direct translocation through the cell membranes, be each internalization pathway more or less favorable to reach the target [17]. Interestingly, the relative contribution of each internalization pathway to the global cellular uptake can depend even on the cell type or the CPP concentration used; therefore, imposing varying cellular barriers (e.g. intracellular stability and/or vesicular sequestration) limit the chances of the cargo to interact with its target [11,17,18]. In line with this, we could speculate that the variable response observed in cancer cells towards CIGB-300 relies on the differential ability of this peptide to circumvent such barriers on each tumor cell to reach the B23/NPM target at its main subcellular localization, the cell nucleolus. Indeed, such findings deserve further experimentation designed to better characterize de-internalization routes and its association with the CIGB-300's response profile on tumor cells.

Here, we validated B23/NPM as a major target for CIGB-300 in tumor cells. At least two other groups are currently targeting such oncogenic protein to induce apoptosis in cancer cells [19,20]. However, CIGB-300 becomes the first compound that by targeting the CK2-mediated phosphorylation on the B23/NPM substrate, exhibits anticancer properties both *in vitro* and *in vivo* [1,9,10,21]. Moreover, at the same time our work provides the first clues to explain the differential antiproliferative response towards CIGB-300 observed in tumor cells. Importantly, such findings suggest that further improvements to this CPP-based drug should entail its more efficient intracellular delivery at the B23/NPM main subcelular localization, the cell nucleus.

Acknowledgements

We thank to Flavio Meggio who generously provided us with the tetrabromobenzotriazole compound and to Glay Chinea for his assistance with chemical structures. This work was supported by C.I.G.B. and Biorec: Grant CIGB-300.

References

1 Perea SE, Reyes O, Puchades Y, Mendoza O, Vispo NS, Torrens I, Santos A, Silva R, Acevedo B, López E, Falcón V, Alonso DF. Antitumor effect of a novel proapoptotic peptide that impairs the phosphorylation by the protein kinase 2 (Casein Kinase 2). *Cancer Res.* 2004; **64**: 7127–7129.
2 Prudent R, Cochet C. New protein kinase CK2 inhibitors: jumping out of the catalytic box. *Chem. Biol.* 2009; **16**: 112–120.
3 Ahmed K, Gerber DA, Cochet C. Joining the cell survival squad: an emerging role for protein kinase CK2. *Trends Cell Biol.* 2002; **12**: 226–230.
4 Duncan JS, Litchfield DW. Too much of a good thing: the role of protein kinase CK2 in tumorigenesis and prospects for therapeutic inhibition of CK2. *Biochim. Biophys. Acta* 2008; **1784**: 33–47.
5 Ruzzene M, Pinna LA. Addiction to protein kinase CK2: a common denominator of diverse cancer cells? *Biochim. Biophys. Acta* 2010; **1804**: 499–504.
6 Wadia JS, Dowdy SF. Transmembrane delivery of protein and peptide drugs by TAT-mediated transduction in the treatment of cancer. *Adv. Drug Deliv. Rev.* 2005; **57**: 579–596.
7 Meggio F, Pinna LA. One-thousand-and-one substrates of protein kinase CK2?. *FASEB J.* 2003; **17**: 349–368.
8 Grisendi S, Mecucci C, Falini B, Pandolfi PP. Nucleophosmin and cancer. *Nat. Rev. Cancer* 2006; **6**: 493–505.
9 Perera Y, Farina HG, Gil J, Rodriguez A, Benavent F, Castellanos L, Gómez RE, Acevedo B, Alonso DF, Perea SE. Anticancer peptide CIGB-300 binds to nucleophosmin/B23, impairs its CK2-mediated phosphorylation, and leads to apoptosis through its nucleolar disassembly activity. *Mol. Cancer Ther.* 2009; **8**: 1189–1196.
10 Perea SE, Reyes O, Baladron I, Perera Y, Farina H, Gil J, Rodriguez A, Bacardi D, Marcelo JL, Cosme K, Cruz M, Valenzuela C, Lopez-Saura PA, Puchades Y, Serrano JM, Mendoza O, Castellanos L, Sanchez A, Betancourt L, Besada V, Silva R, Lopez E, Falcon V, Hernandez I, Solares M, Santana A, Diaz A, Ramos T, Lopez C, Ariosa J, Gonzalez LJ, Garay H, Gomez R, Alonso DF, Sigman H, Herrera L, Acevedo B. CIGB-300, a novel proapoptotic peptide that impairs the CK2 phosphorylation and exhibits anticancer properties both *in vitro* and *in vivo*. *Mol. Cell. Biochem.* 2008; **316**: 163–167.
11 Patel LN, Zaro JL, Shen WC. Cell penetrating peptides: intracellular pathways and pharmaceutical perspectives. *Pharm. Res.* 2007; **24**: 1977–1992.
12 Cell Line Verification Test Recommendations, ATCC Technical Bulletin No. 8 2008.
13 Boyd MR. The NCI in vitro anticancer drug discovery screen: concept, implementation, and operation, 1985–1995, in *Anticancer Drug Development Guide: Preclinical Screening, Clinical Trials, and Approval*. Humana Press, Totowa, NJ USA, 1997.
14 Laemmli UK Cleavage of structural proteins during the assembly of the head of bacteriophage T4. *Nature* 1970; **227**: 680–685.
15 Hallbrink M, Floren A, Elmquist A, Pooga M, Bartfai T, Langel U. Cargo delivery kinetics of cell-penetrating peptides. *Biochim. Biophys. Acta* 2001; **1515**: 101–109.
16 Zorko M, Langel U. Cell-penetrating peptides: mechanism and kinetics of cargo delivery. *Adv. Drug Deliv. Rev.* 2005; **57**: 529–45.
17 Langel U. *Handbook of Cell-Penetrating Peptides*. (Eds.)Taylor & Francis Group. Stockholm, Sweden, 2006; 29–43.
18 Tünnemann G, Martin RM, Haupt S, Patsch C, Edenhofer F, Cardoso MC. Cargo-dependent mode of uptake and bioavailability of TAT-containing proteins and peptides in living cells. *FASEB J.* 2006; **20**: 1775–1784.
19 Qi W, Shakalya K, Stejskal A, Goldman A, Beeck S, Cooke L, Mahadevan D. NSC348884, a nucleophosmin inhibitor disrupts oligomer formation and induces apoptosis in human cancer cells. *Oncogene* 2008; **27**: 4210–4220.
20 Jian Y, Gao Z, Sun J, Shen Q, Feng F, Jing Y, Yang C. RNA aptamers interfering with nucleophosmin oligomerization induce apoptosis of cancer cells. *Oncogene* 2009; **28**: 4201–4211.
21 Perera Y, Farina HG, Hernandez I, Mendoza O, Serrano JM, Reyes O, Gomez DE, Gomez RE, Acevedo BE, Alonso DF, Perea SE. Systemic administration of a peptide that impairs the protein kinase (CK2) phosphorylation reduces solid tumor growth in mice. *Int. J. Cancer* 2008; **122**: 57–62.
22 URL: http://www.celldeath.de/apometh/dnafragm.html [last accessed July 2011]

